

LA-UR-81-898

LA-UR-81-898-2

TITLE: RECENT APPLICATIONS OF  $^{13}\text{C}$  NMR SPECTROSCOPY TO BIOLOGICAL SYSTEMS

**MASTER**

AUTHOR(S): N. A. Matwiyoff

SUBMITTED TO: Proceedings - to be presented at the Conference on Stable Isotopes in Medicine, Agriculture, Geochemistry, Life Sciences, and Environmental Studies, Julich, Fed. Republic of Germany - March 23-26, 1981.

DISCLAIMER

By acceptance of this article, the publisher recognizes that the U.S. Government retains a nonexclusive, royalty free license to publish or reproduce the published form of this contribution, or to allow others to do so, for U.S. Government purposes.

The Los Alamos Scientific Laboratory requests that the publisher identify this article as work performed under the auspices of the U.S. Department of Energy.

University of California



**LOS ALAMOS SCIENTIFIC LABORATORY**

Post Office Box 1663 Los Alamos, New Mexico 87545

An Affirmative Action/Equal Opportunity Employer

# RECENT APPLICATIONS OF $^{13}\text{C}$ NMR SPECTROSCOPY TO BIOLOGICAL SYSTEMS

N. A. Matwiyoff

Los Alamos National Laboratory, University of California

Los Alamos, New Mexico 87545 (U.S.A.)

## Abstract

Carbon-13 nuclear magnetic resonance (nmr) spectroscopy, in conjunction with carbon-13 labeling, is a powerful new analytical technique for the study of metabolic pathways and structural components in intact organelles, cells, and tissues. The technique can provide, rapidly and non-destructively, unique information about: the architecture and dynamics of structural components; the nature of the intracellular environment; and metabolic pathways and relative fluxes of individual carbon atoms. With the aid of results recently obtained by us and those reported by a number of other laboratories, the problems and potentialities of the technique will be reviewed with emphasis on: the viscosities of intracellular fluids; the structure and dynamics of the components of membranes; and the primary and secondary metabolic pathways of carbon in microorganisms, plants, and mammalian cells in culture.

"RECENT APPLICATIONS OF  $^{13}\text{C}$  NMR SPECTROSCOPY  
TO  
BIOLOGICAL SYSTEMS"

INTRODUCTION

Carbon-13 nuclear magnetic resonance (nmr) spectroscopy, in conjunction with carbon-13 labeling, has become an important analytical technique for the study of biological systems and biologically important molecules. The growing list of its well established applications to isolated molecules in solution includes the investigation of: metabolic pathways; the microenvironments of ligands bound to proteins; the architecture and dynamics of macromolecules; the structures of coenzymes and other natural products; and the mechanisms of reactions. Recently interest has been reawakened in the use of the technique for the study of metabolic pathways and structural components in intact organelles, cells, and tissues. The promise and problems in the use of  $^{13}\text{C}$  nmr spectroscopy and  $^{13}\text{C}$  labeling in such investigations can be illustrated by the results of some early work on suspensions of the yeast, *Candida utilis* (1,2).

Reproduced in Fig. 1 is a set of  $^{13}\text{C}$  nmr spectra of a thick suspension of *C. utilis* cells to which  $[1-^{13}\text{C}]$  glucose had been added. (1) These spectra show that, despite the high viscosity and heterogeneity of the suspension, the relaxation times of  $^{13}\text{C}$  are favorable enough to allow the time course to be traced for the anaerobic metabolism of the  $\beta$  and  $\alpha$  anomers of glucose ( $\bullet$ ) to the end product ethanol ( $\alpha$ ). In addition, the spectra revealed that an intermediate metabolite, later identified as trehalose (3), slowly accumulates and eventually is consumed. The  $^{13}\text{C}$  spectrum of the osmotically shocked *C. utilis* cells themselves shown in Fig 2b is also of remarkably high resolution, allowing the assignment of the major resonances to the fatty acid and choline residues of the lipids in the cell membranes and the glycoside residues of the cell wall (1). Later  $^{13}\text{C}$  relaxation time studies (2) of the membranes revealed a gradient of increased mobility from the glycerol backbone of the lipids toward the terminal methyl groups of the fatty acids and the choline head groups, and further that protein-lipid interactions make a negligible contribution to the mobility gradient.

Despite the promise of the technique as revealed by these and other early studies, relatively little work on intact systems was done in the period following. This was due no doubt to a combination of circumstances including: (a) lack of suitably sensitive instrumentation in many laboratories; (b) the scarcity and expense of appropriate  $^{13}\text{C}$  labeled precursors; (c) the limited access of nmr spectroscopists to biochemists and microbiologists who could provide guidance on the selective labeling of the extremely complex cells and tissues (vide infra); and (d) nmr spectroscopists with the appropriate instrumentation were directing their attention to developing a data base for the study of biologically interesting macromolecules. As noted earlier, this situation has begun to change and, in the following discussion, we review briefly recent progress in this rapidly growing field.

#### METABOLIC PATHWAYS

Spurred mainly by the increased availability of sensitive high field  $^{13}\text{C}$  nmr spectrometers, the study of metabolic pathways in intact cells has increased dramatically in recent years. Illustrative examples of this work are summarized in Table I. For the purposes of examining some of the detailed information obtainable in such studies, we will first explore some recent work <sup>(13)</sup> we have been doing with Microbacterium ammoniaphilum and then discuss the significant highlights of the work summarized in Table I.

Our work with Microbacterium ammoniaphilum had its origins in the continuing program at the Los Alamos National Laboratory on the use of microorganisms for the large scale synthesis of natural products, uniformly or specifically labeled with carbon-13. The focus of this research work at present is on those L-amino acids for which efficient organic synthesis methods are not now available and for which there is a need in human metabolic and nutritional studies and in the investigation of the structure and dynamics of enzymes enriched with labeled amino acids. M. ammoniaphilum was one of the microorganisms selected for early study because it produces glutamic acid in a 35-40% yield from glucose and will also use acetate as a substrate for glutamate production (14). In addition to optimizing the incorporation of the  $^{13}\text{C}$  label from glucose or acetate into glutamate, a matter of practical concern to us for some mass spectrometric and nmr studies is the degree to which the label becomes randomized in glutamate due to the flux of glucose and acetate metabolites through various pools.

The major metabolic pathways for glucose and acetate leading to glutamate production in this microorganism are summarized in Fig. 3. As noted in the

figure caption, the flow of  $[1-^{13}\text{C}]$  glucose metabolites to  $\alpha$ -ketoglutarate and glutamate through part of the TCA or GS cycles will result in specifically labeled products but that those formed from intermediates experiencing one or more turns of these cycles will have a more random and complex distribution of the  $^{13}\text{C}$  label. Summarized in Fig. 4 is the time dependence of the  $^{13}\text{C}$  spectra of a suspension of *M. ammoniaphilum* containing  $[1-^{13}\text{C}]$  glucose and near the stationary phase of growth. Since the production of glutamate in large quantities by this microorganism does not begin until that stage is attained (14), the initial growth was accomplished with natural abundance glucose to minimize loss of the  $^{13}\text{C}$  label. In addition to the expected resonances from  $^{13}\text{C}$  enriched bicarbonate, glutamate, succinate, and lactate, the spectra in Fig. 4 exhibit prominent peaks from two unusual  $^{13}\text{C}$  labeled products which are eventually consumed, trehalose and glucosylamine. The accumulation of trehalose, which presumably functions as a storage carbohydrate, has been observed previously by  $^{13}\text{C}$  NMR in growing yeast (1,3) and differentiating amoeba cultures (15). To our knowledge, glucosylamine formation in cell culture has not been observed and, at present, we do not know whether its synthesis is under enzyme control and what role it plays in the control of glucose or nitrogen metabolism. The formation of lactate and succinate by *M. ammoniaphilum* depends on the oxygen tension which, for the cultures appropriate to Fig. 4, fell sharply in the later stages of glucose consumption. As illustrated in Fig. 5, the lactate and succinate levels of fully aerated cultures are sharply reduced.

The C-2, C-3, and C-4 glutamate resonances in Figs. 4 and 5 are predominately singlets suggesting that either: (a) There is a low incorporation of  $^{13}\text{C}$  resulting in a small probability of neighboring  $^{13}\text{C}$ - $^{13}\text{C}$  and  $^{13}\text{C}$ - $^{13}\text{C}$ - $^{13}\text{C}$  occupations whose scalar interactions would result in  $^{13}\text{C}$  multiplets; or (b) The  $^{13}\text{C}$  incorporation is high and results from those biosynthetic pathways discussed earlier, which introduce the label into specific sites with a minimum of randomization. The proton spectrum reproduced in Fig. 6 demonstrates clearly that the latter choice is the correct one. Indeed, the proton NMR data suggest that the  $^{13}\text{C}$  population at C-4 of glutamate (38%) approaches that theoretically possible (45%) if all the ( $[3-^{13}\text{C}$  (45 atom %)] pyruvate resulting from  $[1-^{13}\text{C}$  (90 atom %)] glucose metabolism were incorporated into C-4 via the first third of the Krebs cycle (see captions, Fig. 3). By combining the proton and carbon-13 NMR data and assuming that only the pathways illustrated in Fig. 3 are operative, one can calculate that the relative contribution of the metabolic routes to the labeling of glutamate is that summarized in Fig. 7. A noteworthy aspect revealed

this analysis is that the simultaneous occupation of  $^{13}\text{C}$  at C-2 and C-3 and C-3 and C-4 of glutamate is only possible via multiple turns of the Krebs or glyoxylate cycles. The lack of pronounced multiplets in the  $^{13}\text{C}$  spectra of labeled glutamate rule out the single or multiple turns as predominant events in the processing of glucose metabolites by the cells. This point, which is emphasized further in Fig. 8, should serve as a caution to those who seek to extract labeling probabilities solely from a comparison of multiplet to singlet intensities in  $^{13}\text{C}$  NMR spectra--as we have observed previously (5), the technique generally will work only if the labeling of the carbon atoms giving rise to the multiplet (s) is random. A special case is illustrated in Fig. 9

The studies summarized in Table I address a number of interesting and important questions in metabolism but space will allow only a brief discussion of a few illustrative examples. In the study of Deslaurier et al (12) on the degradation of  $^{13}\text{C}$  labeled enkephalin and enkephalinamide by neuroblastoma X glioma hybrids, the intent was to analyze the conformation of those neuroactive peptides when bound to the opiate receptors of the cells. Instead, and despite reports of successful studies of the binding of enkephalins to neuroblastoma X glioma cells using other techniques, the  $^{13}\text{C}$  NMR studies of [3[2- $^{13}\text{C}$ ] glycine] methionine--enkephalinamide showed unequivocally that the peptide is extensively degraded and the authors concluded that  $^{13}\text{C}$  NMR studies of opioid peptide-receptor interactions will require the use of metabolically stable analogs. The study of Ogino et al (10) on the metabolic regulations and pyruvate transport in anaerobic *E. coli* cells is of special interest because only the signals of metabolites which had diffused through the cell membrane and accumulated in the medium were observed, thus allowing the evaluation of the effect of perturbations to the cell on the influx and egress of pyruvate. In one of the extensive series of studies by Shulman and co-workers (6, 7, 9), an intact mouse liver filling the radio frequency coil space of an nmr spectrometer, was perfused with nutrients containing [3- $^{13}\text{C}$ ] alanine and [2- $^{13}\text{C}$ ] ethanol and the time course of the effects of ethanol on the metabolism of the glucogenic amino acid were studied in detail, including the effect on the flow of the label into various metabolites of: mitochondrial and cytosolic fumarase activity, operation of the pentose cycle; and the activities of glutamine synthetase and pyruvate carboxylase. Considering the utility of the studies discussed above and summarized in Table I, we expect that studies of the metabolism of  $^{13}\text{C}$  labeled substrates in cells, tissues, and organs by  $^{13}\text{C}$  NMR spectroscopy will continue to expand rapidly. Looking to additional

areas of application of the technique in the future, we felt that a particularly promising one is in the area of biochemical genetic analysis of mutant mammalian cells by  $^{13}\text{C}$  tracing experiments to establish the precise site(s) of the biochemical block(s) where  $^{13}\text{C}$  intermediate(s) accumulate in mutants produced by radiation and environmental chemicals.

#### STRUCTURAL COMPONENTS OF INTACT CELLS AND TISSUES

The  $^{13}\text{C}$  spectrum of the *C. utilis* membranes reproduced in Fig. 2b allows one to extract only the average chemical shift and relaxation data for a system which is markedly heterogeneous. Studies of more general utility must make use of selected biosynthetic pathways to label specific sites or structural elements for  $^{13}\text{C}$  nmr investigations on intact cells and tissues or on component reconstituted macromolecular assemblages. Recently there has been an increasing amount of work directed to that end, illustrative examples of which are summarized in Table 2. In an early study (18), mice were kept on a histidine deficient diet supplemented with [2- $^{13}\text{C}$ ] histidine for a red blood cell life time with a consequent specific  $^{13}\text{C}$  enrichment of the histidine residues of the red blood cell hemoglobin. Subsequent  $^{13}\text{C}$  relaxation studies of the hemoglobin within the cell showed that the viscosity of the intracellular fluid is similar to that of water. A similar result was obtained in a related study of frog muscle labeled with  $^{13}\text{C}$  enriched glycine.

In an extensive series of studies, Van Deenen and co-workers (20) were able to highly label the phosphatidylcholine of red blood cell, liver microsome and sarcoplasmic reticulum membranes of rats fed a choline deficient diet supplemented with [ $\text{Me}_3$ - $^{13}\text{C}$ ] choline for a period of eight days.  $^{13}\text{C}$  nmr studies of the muscle microsomes revealed an asymmetric distribution of phosphatidyl choline between the inner (60%) and outer (40%) surfaces of the membranes of the sarcoplasmic reticulum. This asymmetry is opposite to that found for erythrocytes and may be related to the fact that the former are endoplasmic membranes whose outer surface corresponds to the inner surface of plasma membranes. That same group has used reconstituted macromolecular assemblages to study the permeability barriers in large unilamellar glycoporphin containing vesicles of [ $\text{Me}_3$ - $^{13}\text{C}$ ] phosphatidyl choline and have found that the barrier properties of glycoporphin containing bilayers of phosphatidyl choline can be restored by 10 mol % phosphatidylethanolamine or lysophosphatidylcholine.

A final illustration of the broad range and great promise of the experiments being conducted in this area is the study of de Wit and co-workers (21) who

enriched tobacco mosaic virus and its proteins to the 12 atom %  $^{13}\text{C}$  level using  $^{13}\text{CO}_2$  as the carbon source. In addition to developing some interesting conclusions about the interaction between RNA and protein, these workers observed that the double disks formed by the proteins in the absence of RNA contain mobile  $^{13}\text{C}$  atoms at all sites within the disks which were formed in solutions of .1-.2 ionic strengths. In contrast, X-Ray data for crystals of stacks of double disks obtained from 0.8 ionic strength solutions indicate that the motion of the carbon atoms is highly restricted. Thus there are important structural differences between the crystals studied by X-Ray and the disks formed in solution near the physiological ionic strength, a conclusion strengthened by the NMR observation that there is an increasing degree of immobilization of the carbon atoms in the double disklike oligomers as the ionic strength increases.

#### ACKNOWLEDGMENT

The author is grateful for helpful discussions of the glutamate biosynthesis with Drs. R. E. London and T. E. Walker and for their participation in the design Figs. 3-9. This work was done under the auspices of the U. S. Department of Energy.



REFERENCES

1. R. T. Eakin, L. O. Morgan, C. T. Gregg, and N. A. Matwiyoff, FEBS Letts, 28 259-263 (1973).
2. R. E. London, V. H. Kollman, and N. A. Matwiyoff, Biochem, 14, 5492-5000 (1975).
3. M. Kainosho, K. Ajisaka, and H. Nakazawa, FEBS Letts, 80, 385-389 (1977).
4. (a) J. Schaefer, E. O. Stejskal, and C. F. Beard, Plant Physiol, 55, 1048 (1975); see also (b) J. Schaefer, E. O. Stejskal, and R. A. McKay, Biochem. Biophys. Res. Commun., 88, 274-280, (1979).
5. (a) R. E. London, V. H. Kollman, N. A. Matwiyoff, and D. D. Mueller, Proc. Sec. Intl. Conf. Stable Isotopes (E. R. Klein and P. D. Klein, ed.) U. S. Energy Research and Development Report CONF-751027 (1976), pp 470-484.  
also (b) V. H. Kollman, J. L. Hanners, R. E. London, E. G. Adame, and T. E. Walker, Carbohydr. Res., 73 193-202 (1979).
6. K. Ugurbil, T. R. Brown, J. A. Den Hollander, P. Glynn, and R. G. Schulman, Proc Natl. Acad Sci (USA), 75, 3742-3746 (1978).
7. J. A. Den Hollander, T. R. Brown, K. Ugurbil, and R. G. Shulman, Proc. Natl. Acad Sci (USA), 76, 6096-6100 (1979).
8. A. I. Scott, G. Burton, and P. E. Fagerness, J. Chem. Soc. (Chem. Commun.), 199-202 (1979).
9. (a) M. Cohen, S. Ogawa, and R. G. Schulman, Proc. Natl. Acad Sci (USA), 76, 1603-1607 (1979); see also (b) M. Cohen, R. G. Shulman, and A. C. Malachuk, ibid, 76, 4808-4812 (1979).
10. T. Ogino, Y. Arata, and S. Fujiwara, Biochem, 19, 3684-3691 (1980).
11. P. Styles, C. Grathwohl, and F. F. Brown, J. Magn. Res., 35, 329-336 (1979).
12. R. Deslaurier, H. C. Jarrell, D. W. Griffith, W. H. McGregor, and I.C. P. Smith, Int. J. Peptide Protein Res., 16 487-493 (1980).
13. T. E. Walker, C. H. Han, V. H. Kollman, R. E. London, and N. A. Matwiyoff, work in progress.
14. S. Kinoshita, "Glutamic Acid", in The Microbial Production Of Amino Acids, John Wiley and Sons, Inc. N. Y., E. Yamada, S. Kinoshita, T. Tsunoda, and K. Aida, eds., 1972, Chapter 10, pp 263-324.
15. R. Deslaurier, H. C. Jarrell, R. A. Byrd, and I.C.P. Smith, FEBS Lett, 118, 185-190 (1980).
16. J. C. Metcalfe, N. J. M. Birdsall, and A. G. Lee, FEBS Lett, 21, 335 (1972).
17. W. Stoffel and K. Bister, Biochem, 14, 2841 (1975).

18. R. E. London, C. T. Gregg, and N. A. Matwiyoff, Science, 188, 266 (1975).
19. I. C. P. Smith, Can. J. Biochem., 57, 1-14 (1979).
20. A. M. H. P. Van Den Besselaar, B. DeKruijff, H. Van Den Bosch, and L. L. M. Van Deenen, Biochim Biophys Acta, 555, 193-199 (1979); B. De Kruijff, A. M. H. P. Van Den Besselaar, A. Van Den Bosch, and L. L. M. Van Deenen, ibid, 181-192 (1979); W. J. Gerritsen, E. J. J. Van Zoelen, A. J. Verkley, B. De Kruijff, and L. L. M. Van Deenen, ibid, 551, 248-259 (1979).
21. M. C. Neville and H. R. Wyssbrod, Biophys. J., 17, 255-267 (1977).
22. J. L. de Wit, H. C. M. Alma-Zeestraten, M. A. Hemmings, and T. J. Schaafsma, Biochem., 18, 3973-3976 (1979).
23. S. Weinstein, B. A. Wallace, E. R. Blout, J. S. Morrow, and W. Veatch, Proc. Natl. Acad. Sci. (USA), 76, 4230-4234 (1979); B. A. Wallace and E. R. Blout, ibid, 76, 1775-1779 (1979).
24. B. De Kruijff, A. Rietveld, and C. J. A. Van Echteld, Biochim Biophys. Acta, 600, 597-606 (1980).
25. S. Geller, S. C. Wei, G. K. Shkuda, D. M. Marcus, and C. F. Brewer, Biochem., 19, 3614-3623 (1980).
26. P. L. Yeagle, Biochim Biophys Acta, 640, 263-273 (1981).

TABLE I  
ILLUSTRATIVE  $^{13}\text{C}$  NUCLEAR MAGNETIC RESONANCE STUDIES OF METABOLISM IN INTACT CELLS AND TISSUES

System	$^{13}\text{C}$ Labeled Substrate	Observations	Reference
Soybean	$^{13}\text{CO}_2$	Early Label Appears in Sugars and Lipids; At Later Stages Of Metabolism, Sugar Label Is Shuttled Into Lipids.	4a
Anacystis nidulans, Blue Green Alga	$^{13}\text{CO}_2$	Significant Dark Respiration Contributes To The $\text{CO}_2$ Pool Available For The Synthesis Of Galactosyl Glycerol.	5a
Escherichia coli, Bacterium; Saccharomyces cerevisiae, Yeast	[1- $^{13}\text{C}$ ] Glucose and [6- $^{13}\text{C}$ ] Glucose	Different Rates for $\alpha$ - And $\beta$ -Glucose Translocation; Flux Of Carbon Through Most Glycolysis Intermediates To End Products Evaluated; $\alpha$ - and $\beta$ - Fructose Biphosphates Are In Anomeric Equilibrium; in Yeast, But Not In Bacterium, Aldolose-Triose Phosphate Isomerase Triangle Is Near Equilibrium.	6,7
Rhodospseudomonas spheroides; Propionibacterium shermanii	[5- $^{13}\text{C}$ ] AminoLevulinic Acid (ALA) [11- $^{13}\text{C}$ ] Porphobilinogen (PBG)	Direct Demonstration Of Porphyrinogen Intermediates In Porphyrin Biosynthesis.	8
Rat Hepatocytes, normal and Hyperthyroid	[2- $^{13}\text{C}$ ] Glycerol, [1,3- $^{13}\text{C}_2$ ] Glycerol, and [3- $^{13}\text{C}$ ] Alanine	Gluconeogenesis From Alanine And Glycerol; Hyperthyroid Rat Cells Show An Increased Activity Of Mitochondrial Glycerol Phosphate Dehydrogenase Resulting in Enhanced Gluconeogenesis.	9a
Escherichia coli	[1- $^{13}\text{C}$ ] Glucose	Uptake And Efflux Of Pyruvate Affected By pH Of Medium And Will Occur Against Osmotic Gradient. Proton Conductive Uncouplers Inhibit Pyruvate Uptake.	10

TABLE I (contd.)

System	<sup>13</sup> C Labeled Substrate	Observations	Reference
Erythrocytes	[1- <sup>13</sup> C] Glucose	Label From Glucose Incorporated Into Diphosphoglycerate And Lactate.	11
Neuroblastoma X Glioma Cells	[3(2- <sup>13</sup> C)-Glycine] Methionine-Enkephalinamide	Cells Degrade Enkephalinamide To A Mixture Of Peptides And Free Glycine.	12

TABLE II  
ILLUSTRATIVE  $^{13}\text{C}$  NUCLEAR MAGNETIC RESONANCE STUDIES OF  $^{13}\text{C}$  LABELED MACROMOLECULAR ASSEMBLAGES

System	$^{13}\text{C}$ Labeled Precursor	Observations	Reference
<u>Acholeplasma</u> membrane	[1- $^{13}\text{C}$ ] Palmitic Acid	Bulk Membrane Lipids Behave As If In Simple Bilayer Structures.	16
Vesicular Stomatitis Virions	[11- $^{13}\text{C}$ ] Oleic Acid [Me- $^{13}\text{C}$ ] Choline	Motions Of Lipids In Virion Envelope Are More Restricted Than Those In Liposomes.	17
Mouse Erythrocytes	[2- $^{13}\text{C}$ ] Histidine	Intracellular Viscosity Experienced By Hemoglobin Is Only Slightly Higher Than That Of Water.	18
<u>Sarcosodium pullulans</u>	[1- $^{13}\text{C}$ ] And [2- $^{13}\text{C}$ ] Acetic Acid	Dynamic Behavior Of Membrane Lipids Similar To That In Model Membranes.	19
Sarcoplasmic Reticulum Membranes	[Me- $^{13}\text{C}$ ] Choline	Asymmetric Distribution Equilibrium of Lysophosphatidyl Choline Between Inner And Outer Sarcoplasmic Reticulum Membranes Is Established Rapidly.	20
Frog Muscle	[1- $^{13}\text{C}$ ] Glycine	Motion Of Glycine Provides No Evidence For Special Organization Of Intracellular Water.	21
Tobacco Mosaic Virus	$^{13}\text{CO}_2$	Significant Rotational Motion Occurs For Proteins Within TMV And In Protein Oligomers.	22
Phospholipid Vesicles	[ $^{13}\text{C}$ ] Peptides	Gramicidin Channel In Phosphatidyl Choline Vesicles Consists Of An $\text{NH}_2$ -Terminal To $\text{NH}_2$ -Terminal Dimer.	23
Rat Erythrocyte, Endoplasmic, And Sarcoplasmic Reticulum Membranes	[Me- $^{13}\text{C}_3$ ] Choline	$^{13}\text{C}$ Line Widths Of Erythrocyte Membrane Lipids Are Typical For A Lamellar Arrangement But For Endoplasmic Reticulum Membranes Lipid Line Widths Are Small and Characteristic of Isotropic Phases.	24

TABLE II (contd.)

System	$^{13}\text{C}$ Labeled Precursor	Observations	Reference
Fab' Fragments of Anti-poly(L-Alanine) Antibodies	(Me- $^{13}\text{C}_4$ ) Tetra-L-Alanine	$^{13}\text{C}$ Line Widths Indicate That Methyl Groups Of The Tetrapeptide Are Free to Rotate In The Antibody-Hapten Complex With The Peptide Backbone Firmly Bound And In The Slow Exchange Limit	25
Phospholipid Vesicles	(4- $^{13}\text{C}$ ) Cholesterol	Cholesterol Relaxation Data Are Consistent With A $10^{-10}$ S Correlation Time For Axial Rotation In The Vesicle While The Axial Rotation Of The Phospholipid Molecule Is 10-100 Times Slower	26

# FIGURE CAPTIONS

- Fig. 1. Proton Noise Decoupled, Fourier Transform  $^{13}\text{C}$  NMR (25.2 MHz) Spectra Obtained During Metabolism of the  $\beta$ - and  $\alpha$ -Anomers of  $[1-^{13}\text{C}]$  Glucose ( $\bullet$ ) to  $[2-^{13}\text{C}]$  Ethanol ( $\blacksquare$ ) with the Intermediate Formation of  $[1,1'-^{13}\text{C}]$  Trehalose ( $\blacktriangle$ ) by a Suspension of *C. utilis* Cells; And Plots of the Relative Intensities of the Labeled Glucose Ethanol, and Trehalose Resonances as a Function of Time: a) 500 pulses, 3-7 min. after initiation of metabolism; b) 500 pulses, 12-16 min.; c) 1500 pulses, 28-42 min.; d) 1500 pulses, 56-70 min.; e) 1500 min., 83-99 min. Spectra obtained during the initial time period exhibited only the resonances ( $\bullet$ ) corresponding to the C-1 of the  $\beta$ - and  $\alpha$ - anomers of the substrate  $[1-^{13}\text{C}]$  glucose. Spectra obtained in the time periods (d) and (e) exhibited prominent resonances corresponding to C-1 of trehalose ( $\blacktriangle$ ) and C-2 of ethanol ( $\blacksquare$ ) together with natural abundance signals of glucose and *C. utilis* cells, and  $^{13}\text{C}$  enriched resonances of transient intermediates. Due to the low sensitivity, these could not be identified unequivocally.
- Fig. 2. Proton Noise Decoupled Fourier Transform  $^{13}\text{C}$  NMR (25.2 MHz) Spectra of *Candida Utilis* Cells Enriched to the 20 atom % Level with  $[1,2-^{13}\text{C}_2]$  (20 atom %) Acetate: (a) Cells Suspended in  $\text{D}_2\text{O}$ , 995 pulses; (b) Cellular components remaining after exhaustive extraction with  $\text{D}_2\text{O}$ , 10,000 pulses; and (c) Water soluble components released by the osmotic shock of (b), 1082 pulses.
- Fig. 3. Major Metabolic Pathways in *M. ammoniaphilum* Involving Glucose, Acetate, and Glutamate. Glucose Labeled at C-1 produces  $[3-^{13}\text{C}]$  pyruvate via the Embden-Meyerhof pathway (EMP) and unlabeled pyruvate via the hexose monophosphate shunt (HMS).  $[3-^{13}\text{C}]$  pyruvate enters the tricarboxylic acid (TCA) and glyoxylate shunt (GS) cycles as  $[3-^{13}\text{C}]$  oxaloacetate and/or  $[2-^{13}\text{C}]$  acetate and can result in the formation of  $[2-^{13}\text{C}]$  glutamate,  $[4-^{13}\text{C}]$  glutamate, and  $[2,4-^{13}\text{C}]$  glutamate via  $\alpha$ -ketoglutarate formed in a third of a turn of the TCA cycle. Formation of glutamate after one or more turns of the TCA cycle will tend to randomize the label because of the formation of the symmetrical intermediates succinate and fumarate. In particular, C-4 and C-3 will interchange in one turn, as will C-2 and C-1. Similar scrambling will occur through the flow of citrate through the glyoxylate cycle.
- Fig. 4. Time Dependence Of The Proton Decoupled Fourier Transform  $^{13}\text{C}$  NMR Spectrum (25.2 MHz) Of A Suspension Of *M. ammoniaphilum* Initially Containing  $[1-^{13}\text{C}]$  (90 atom %) Glucose: T-1 hr., spectrum obtained during the 0-2 hr. metabolism period; T-8 hr., during the 7-9 hr. period; and T-20.5 hr., during the 19.5-21.5 period. Enriched  $^{13}\text{C}$  resonances are:  $\text{HCO}_3^-$  ion; Glc, C (97.0 ppm) and C' (93.4 ppm)-C-1 of  $[1-^{13}\text{C}]$  glucose; T (94.2 ppm), C-1 of  $[1,1'-^{13}\text{C}_2]$  trehalose; Glu, C-2 (56.0), C-4 (34.6) and C-3 (28.3) of glutamate; S, C-2,3 (35.3) of succinate; L, C-3 (21.3) of lactate; and GA, B (86.2) and (84.1) C-1 of glucosylamine. In the T-1 hr. and 8 hr. spectrum the glucose C-1 resonances are truncated and the natural abundance glucose resonances are apparent.

- Fig. 5. Time Dependence Of The Proton Decoupled Fourier Transform  $^{13}\text{C}$  NMR Spectra (25.2 MHz) Of The Supernate Of Fully Aerated *M. ammoniaphilum* In Cultures Initially Grown On  $[1-^{13}\text{C}$  (90 atom %)] Glucose. Samples were withdrawn from the cultures and the cells removed by centrifugation at the times indicated. See also the caption to Fig. 4.
- Fig. 6. Proton NMR Spectram (360 MHz) of  $[1,2,3,4-^{13}\text{C}_4]$  Glutamate Derived From *M. ammoniaphilum* Grown On  $[1-^{13}\text{C}$  (90 atom %)] Glucose. For each proton, the center of the multiplet arises from  $^{12}\text{C}$ -H moieties with fine structure caused by H-H scalar interactions. The doublets with similar fine structure are due to the  $^{13}\text{C}$ -H splitting from moieties containing the  $^{13}\text{C}$  label. The  $^{13}\text{C}$  populations calculated from the ratio of the doublet to the singlet intensities are: C-2, 34%; C-3, 38%; and C-4, 14%.
- Fig. 7. Labeling Pathways For The Incorporation Of  $^{13}\text{C}$  Into C-2, C-3, And C-4 Of L-Glutamate Derived From D- $[1-^{13}\text{C}]$  Glucose. Abbreviations are: PEP, phosphoenalpyruvate; OAA, oxaloactate; and Inten, the fractional population of  $^{13}\text{C}$  at the site designated. The data are consistent also with studies of  $[6-^{13}\text{C}]$  glucose. The results are averages, there being evidence of a time dependence of the relative contributions.
- Fig. 8. Proton Decoupled  $^{13}\text{C}$  NMR Spectrum (25.2 MHz) of  $[1,2,3,4-^{13}\text{C}_4]$  Glutamate Derived From *M. ammoniaphilum* Grown On  $[1-^{13}\text{C}$  (90 atom %)] Glucose. The spectrum illustrates the non-random distribution of the  $^{13}\text{C}$  label among the C-2, C-3, and C-4 sites. If the label were distributed randomly with the  $^{13}\text{C}$  abundances derived from the spectra in Fig. 6 then, for example, the C-1 and C-2 signals should consist of approximate 1:2:1 multiplets.
- Fig. 9. Proton Decoupled  $^{13}\text{C}$  NMR (25.2 MHz) Spectrum Of  $[1,5-^{13}\text{C}_2]$  Glutamate Obtained From *M. ammoniaphilum* Grown On  $[1-^{13}\text{C}$  (70 atom %)] Acetate. The cells were grown on natural abundance glucose for 24 hrs. and then transferred to the medium containing  $[1-^{13}\text{C}]$  acetate and cultured for an additional 96 hrs. Only C-1 and C-5 are labeled. From the multiplet to singlet intensities of C-4, the  $^{13}\text{C}$  enrichment at C-5 is calculated to be 70 atom %. From the corresponding intensities for the C-2 resonance, the  $^{13}\text{C}$  enrichment at C-1 is calculated to be ~35 atom %. Dilution of the label at C-2 occurs through decarboxylation in one turn of the TCA cycle.



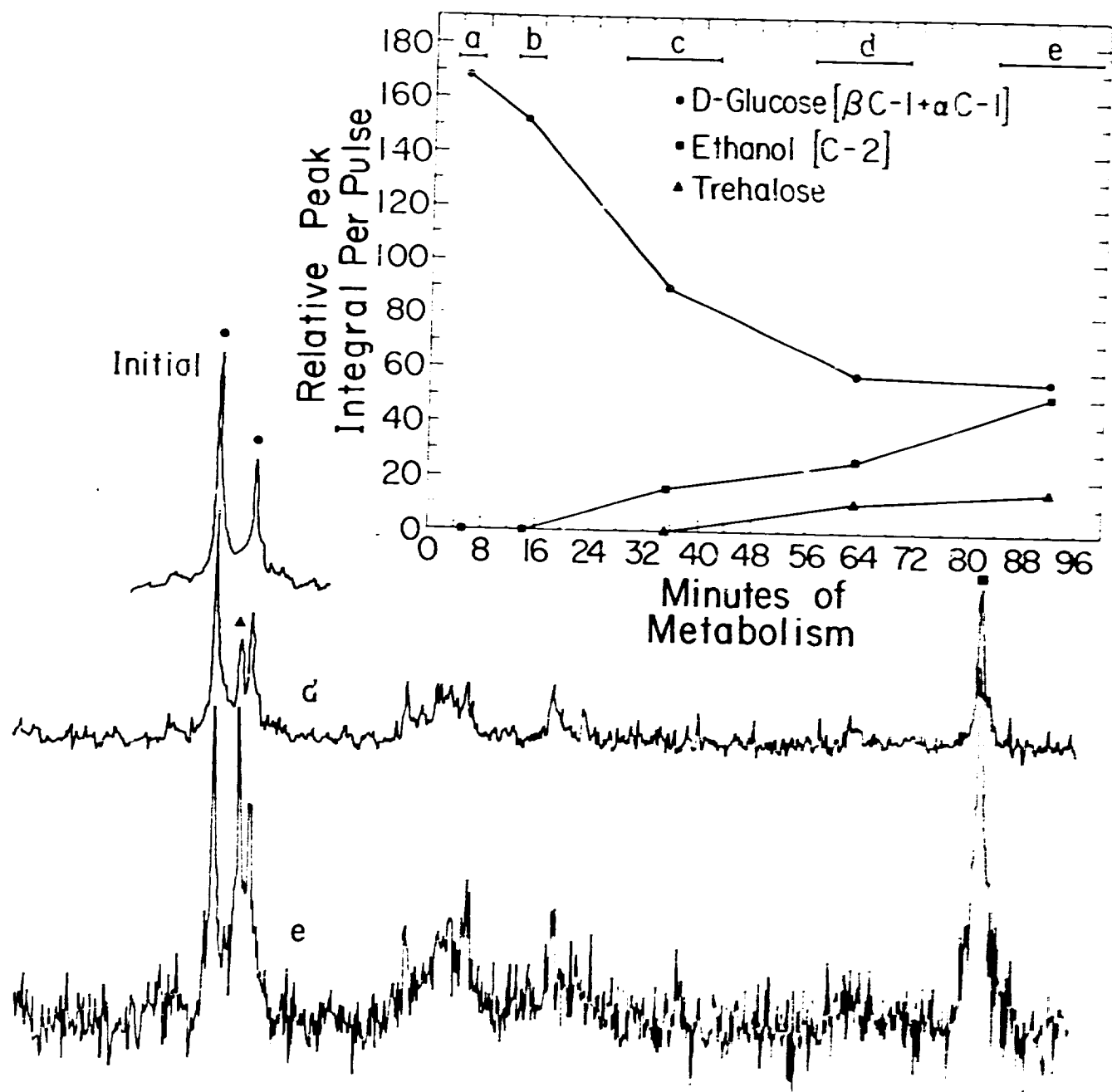


Fig. 1

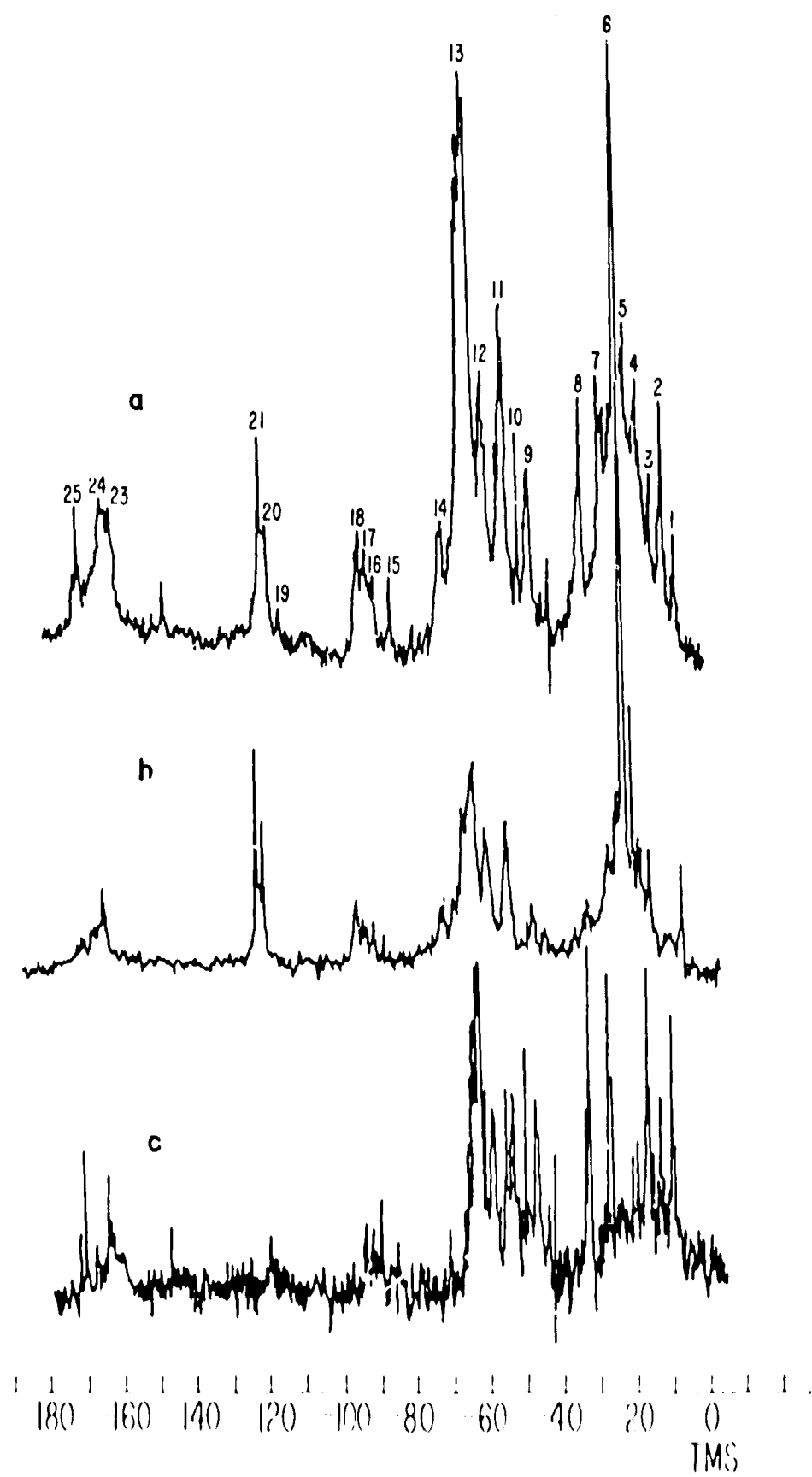


Fig. 2

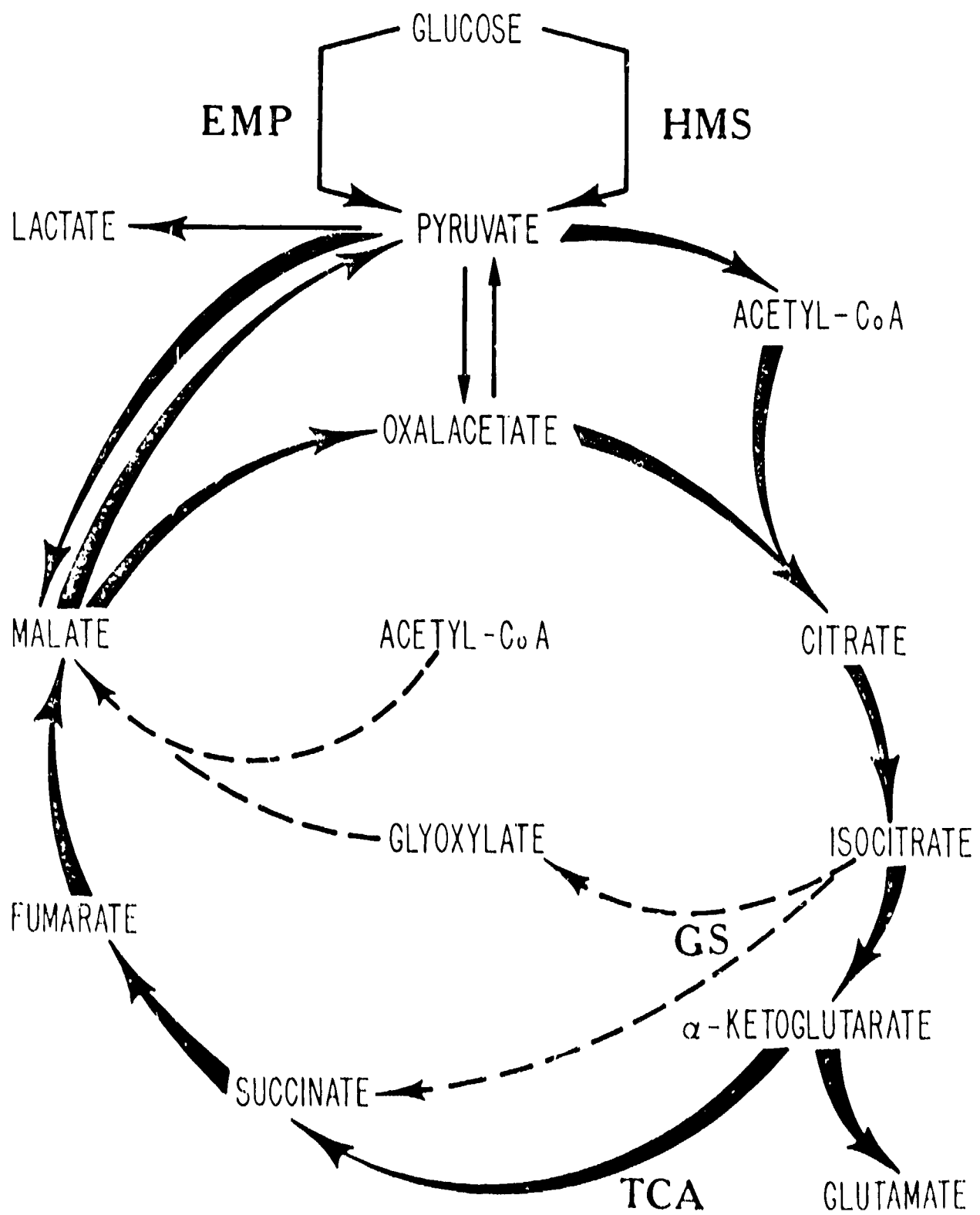


Fig. 3

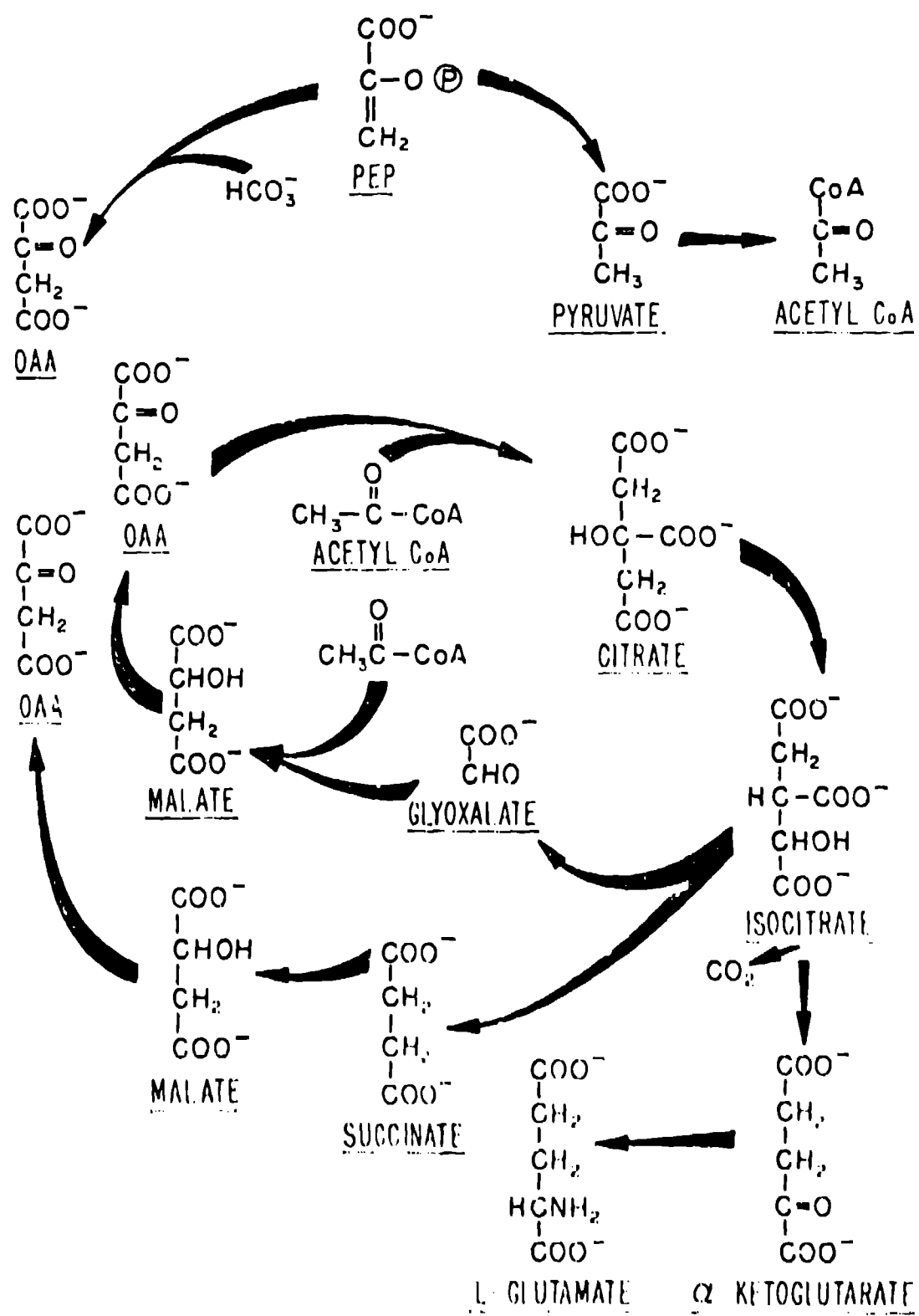


Fig. 3

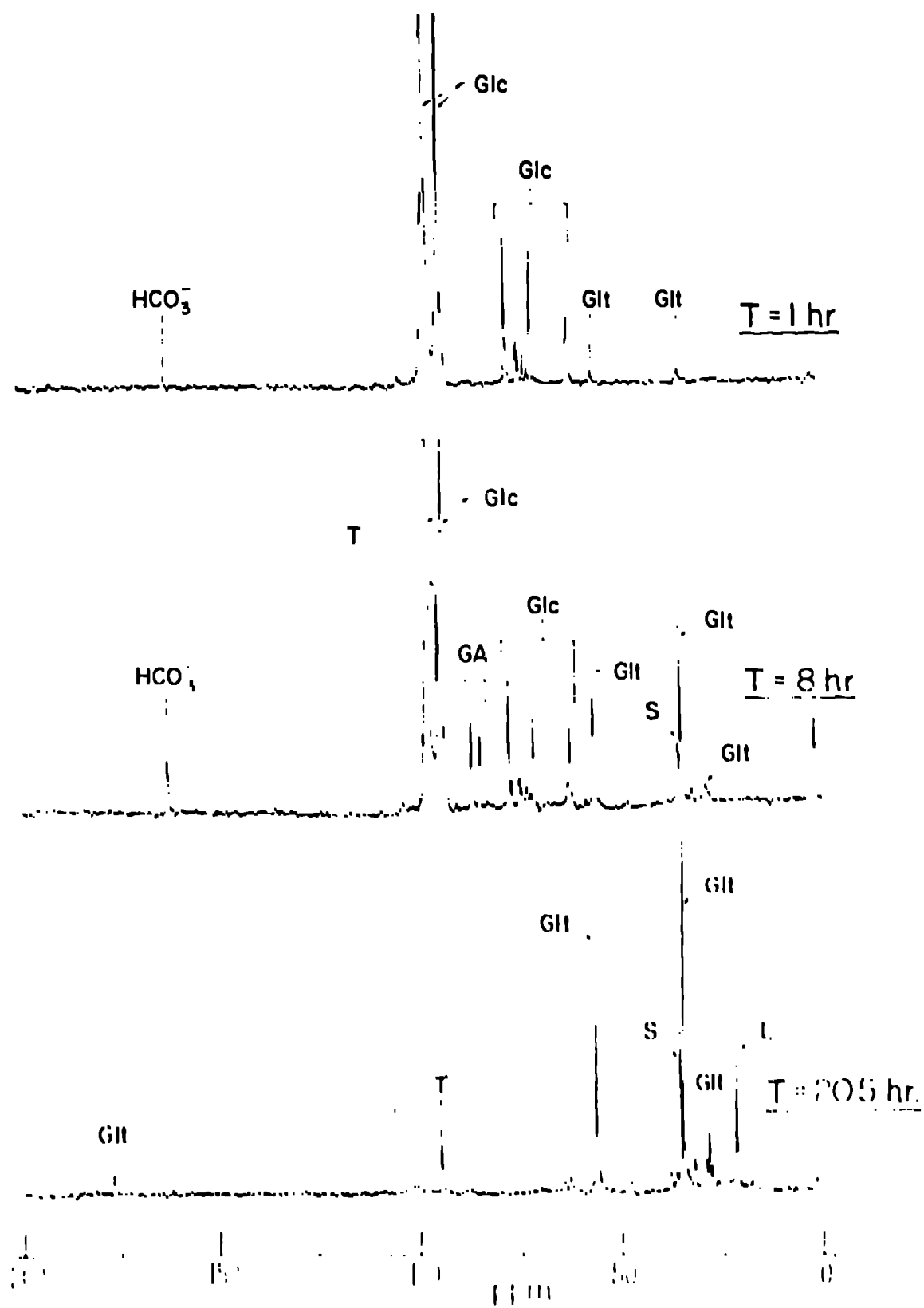


Fig. 4

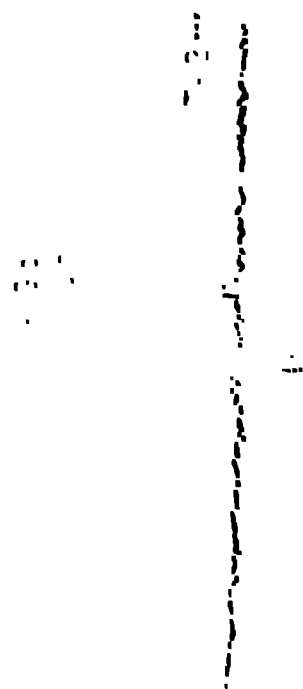
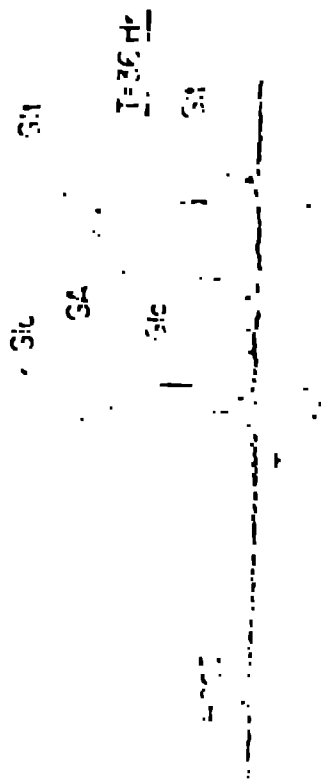
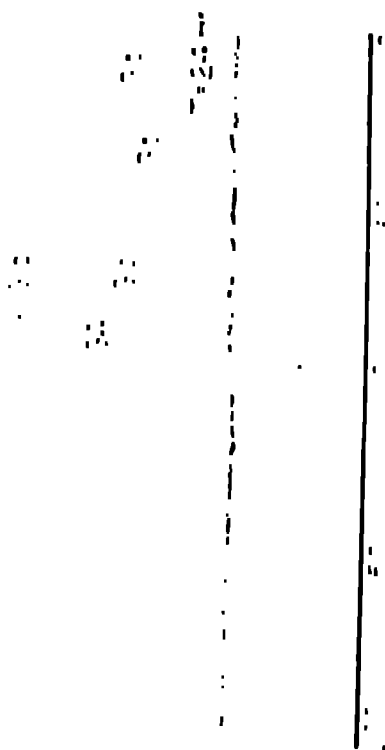
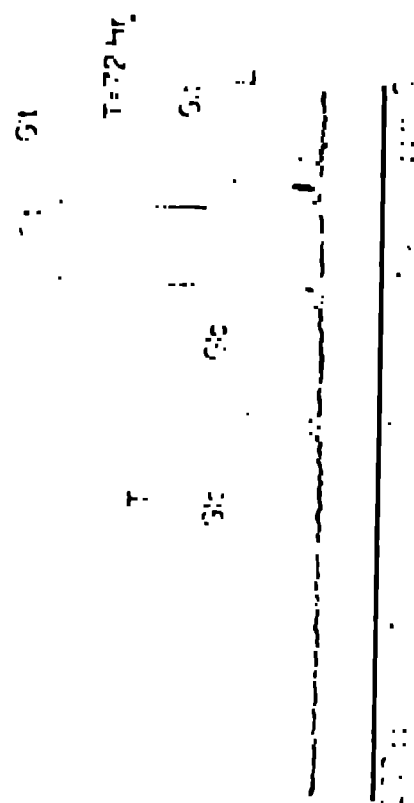


Fig. 5



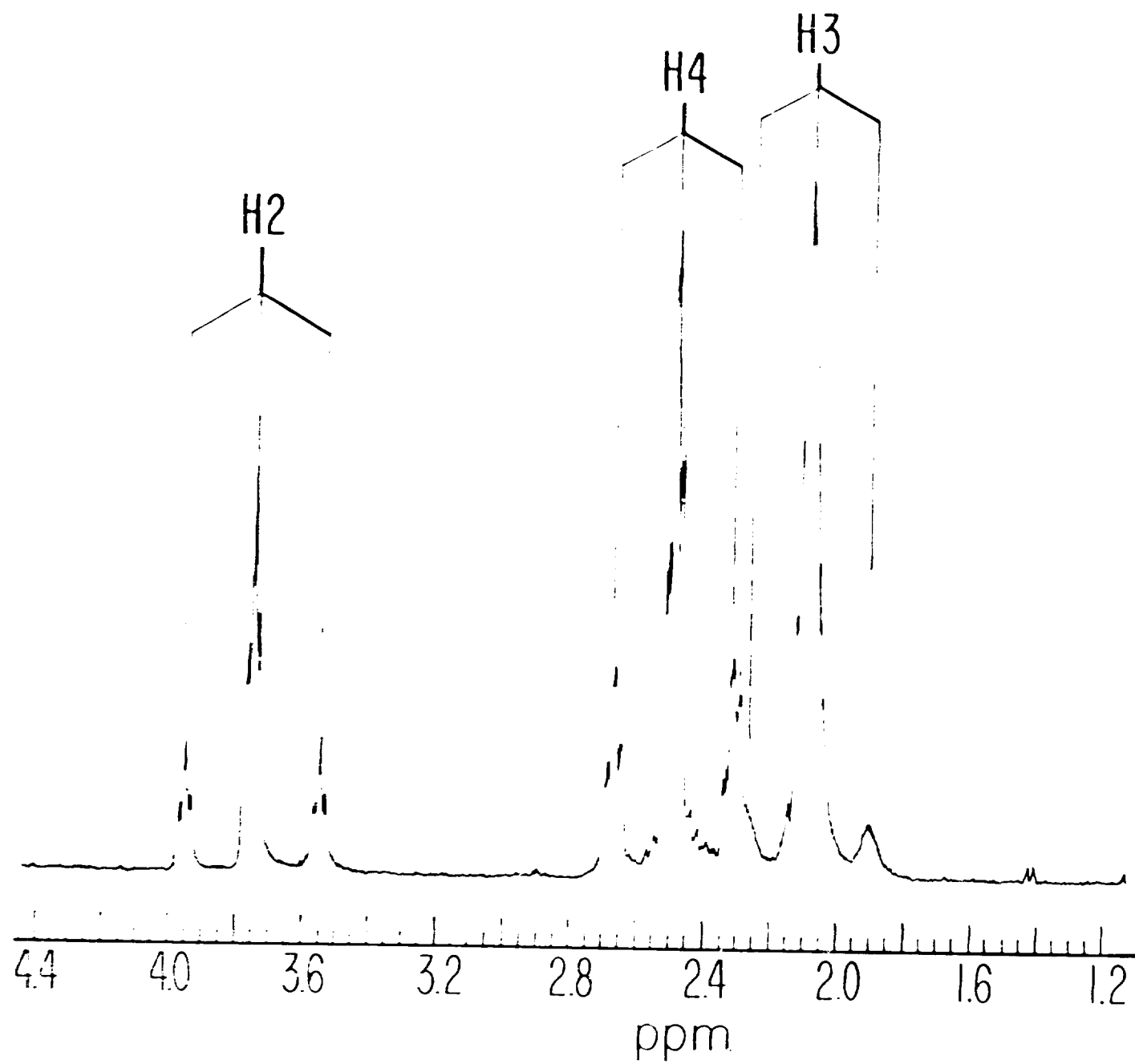


Fig. 6

POSSIBLE LABELING PATTERNS FOR C-2 C-3 AND C-4  
OF L-GLUTAMATE DERIVED FROM D - [1 - <sup>13</sup>C] GLUCOSE

<u>Pathway Designation</u>	<u>Labeling Pattern</u>	<u>Source of Labeling</u>	<u>Pathway %</u>
X	$\overset{*}{C}_2 - C_3 - \overset{*}{C}_4$	PEP → OAA → Glutamate Via 1st third of Krebs Cycle	60%
Y	$\overset{*}{C}_2 - C_3 - \overset{*}{C}_4$ $C_2 - \overset{*}{C}_3 - \overset{*}{C}_4$	Single turn of the Krebs or Glyoxalate cycle	30%
Z	$\overset{*}{C}_2 - \overset{*}{C}_3 - \overset{*}{C}_4$	Multiple turns of the Krebs or Glyoxalate cycle	10%

$$C-2 \text{ Intensity} = \alpha (x + Y/2 + Z)$$

$$C-3 \text{ Intensity} = \alpha (Y/2 + Z)$$

$$C-4 \text{ Intensity} = \alpha (x + Y + Z)$$

$$\text{Normalize} \quad X + Y + Z = 1$$

LOS ALAMOS NATIONAL LABORATORY



Fig. 8

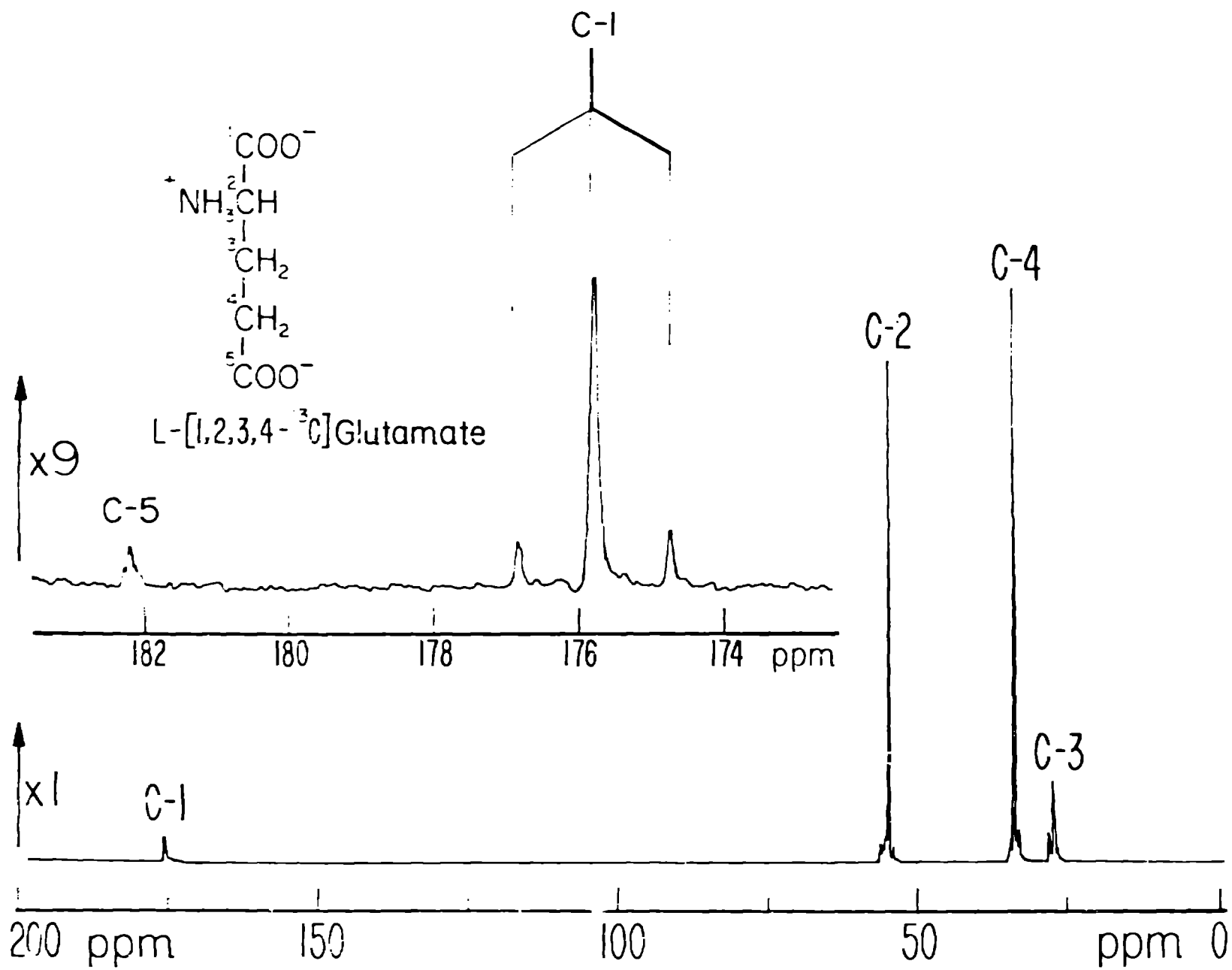


Fig. 9

